UCLA Jet Propulsion Laboratory
California Institute of Technology

Water Vapor Budget in Atmospheric Rivers: A Multi-model Evaluation

Bin Guan[1,2], Duane Waliser[2], and Marty Ralph[3]
[1]Joint Institute for Regional Earth System Science and Engineering, UCLA
[2]NASA Jet Propulsion Laboratory, Caltech
[3]Scripps Institution of Oceanography, UC San Diego

With key input from **Joel Norris** (SIO) and **Guang Zhang** (SIO)

43rd Annual Climate Diagnostics and Prediction Workshop, Santa Barbara, CA, 2018.10.23

Water Vapor, Precipitation, and Atmospheric Rivers
February 2017

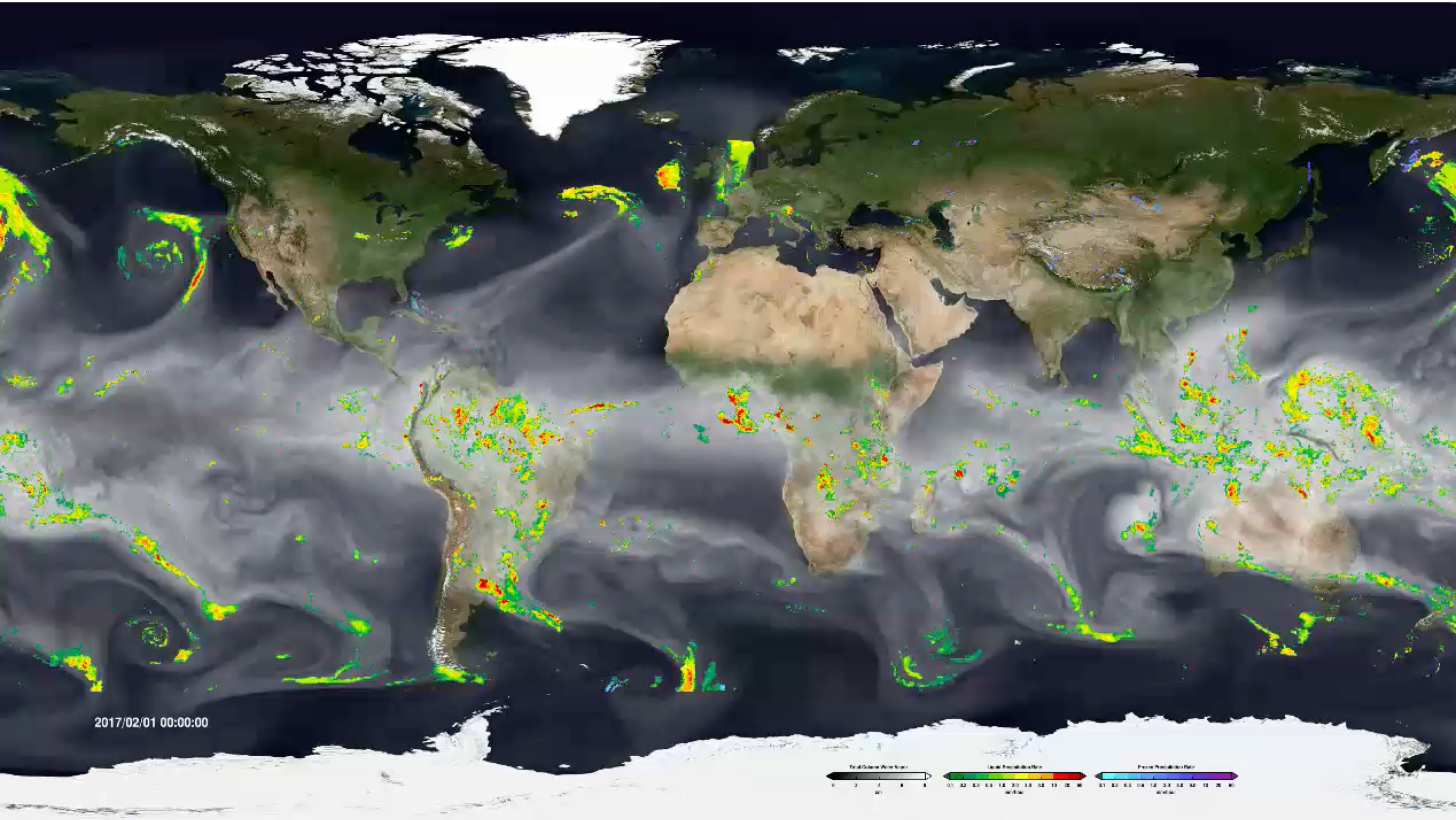

Visualization by NASA/Goddard Space Flight Center Scientific Visualization Studio

Definition of Atmospheric River (AR)

Zhu and Newell (1994):

Filamentary structure is a common feature of atmospheric water vapor transport; the filaments may be termed "atmospheric rivers" bacause some carry as much water as the Amazon.

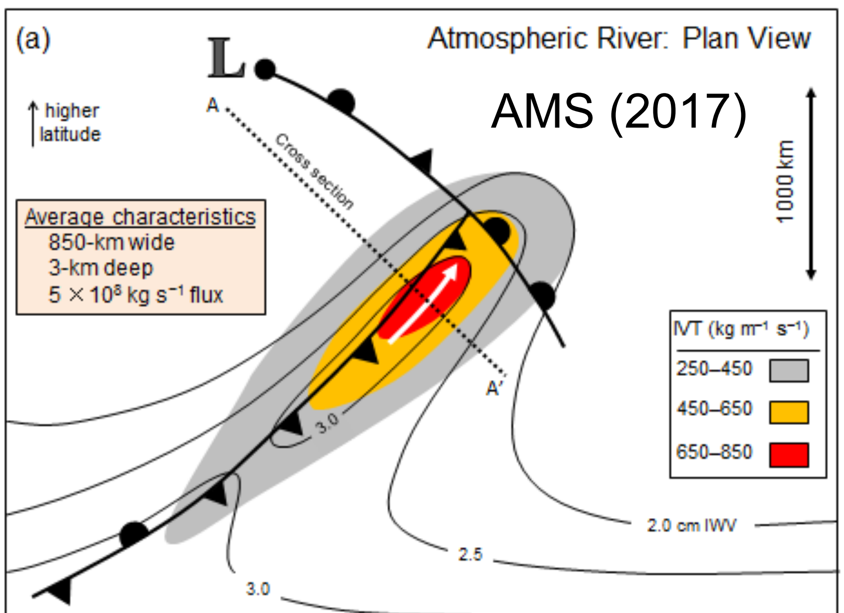

Glossary of Meteorology, AMS (2017):

A long, narrow, and transient corridor of strong horizontal water vapor transport that is typically associated with a low-level jet stream ahead of the cold front of an extratropical cyclone. The water vapor in atmospheric rivers is supplied by tropical and/or extratropical moisture sources. Atmospheric rivers frequently lead to heavy precipitation where they are forced upward—for example, by mountains or by ascent in the warm conveyor belt. Horizontal water vapor transport in the midlatitudes occurs primarily in atmospheric rivers and is focused in the lower troposphere.

ARs are recognized as a particular type of extreme storms in NCA4 CSSR

CSSR Executive Summary: The frequency and severity of landfalling "atmospheric rivers" on the U.S. West Coast … will increase as a result of increasing evaporation and resulting higher atmospheric water vapor that occurs with increasing temperature. (*Medium confidence*) (Ch. 9)

Key Motivations for This Study

- Process-level understanding of ARs; specifically, reanalysis depiction of AR water budgets and uncertainties
- AR water budget in global weather/climate models
- How water budget process-level biases relate to biases in bulk characteristics of ARs (e.g., frequency, geometry, …)

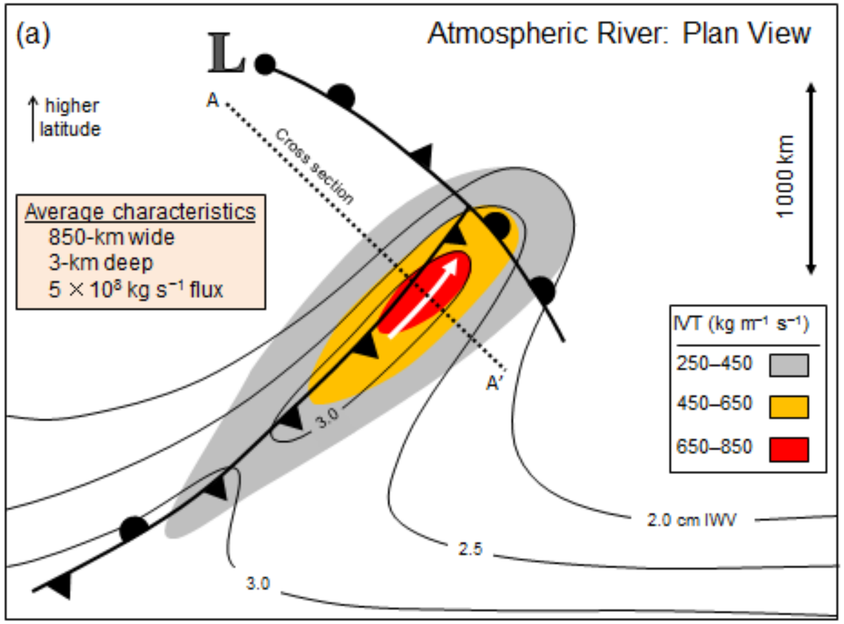

Global AR Detection Algorithm

Refined/enhanced from Guan and Waliser (2015)

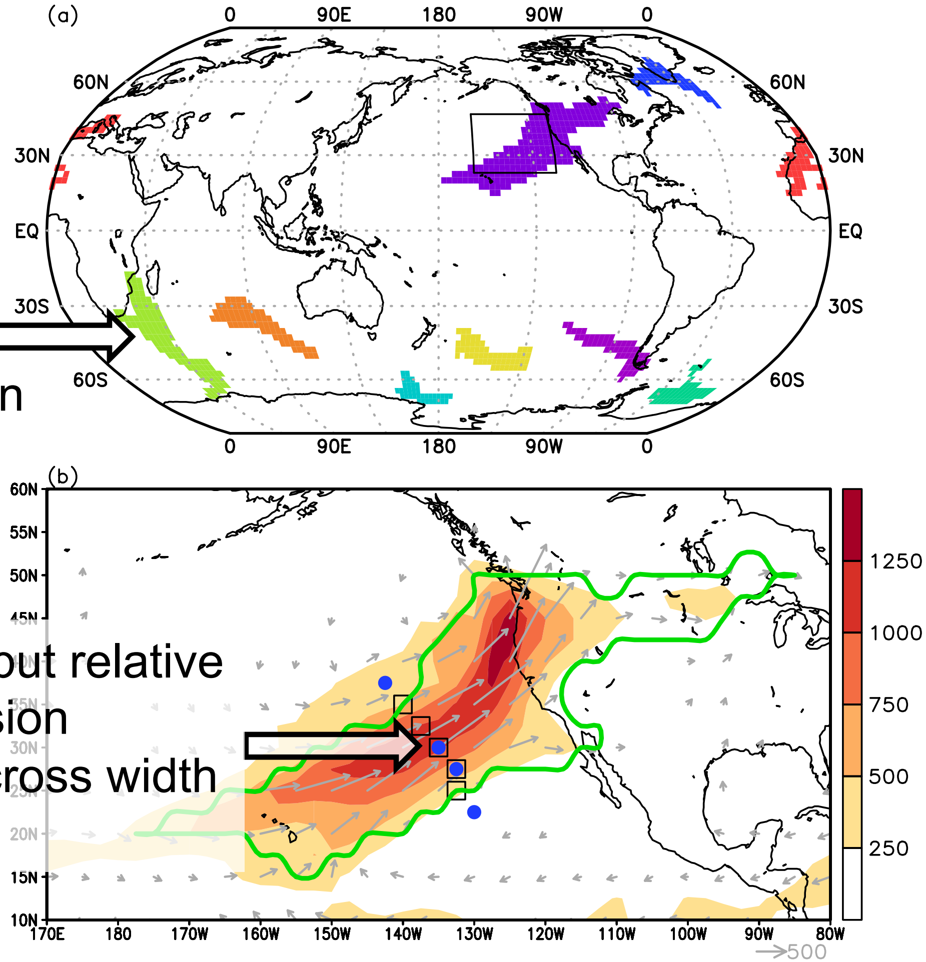

“New” AR
(i.e., undetected in original version)

Enhanced output relative to original version

- Transect across width
- 4 sectors

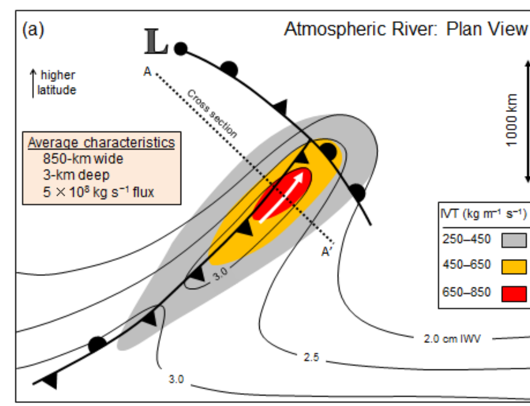

Guan, Waliser, and Ralph (2018a,b)

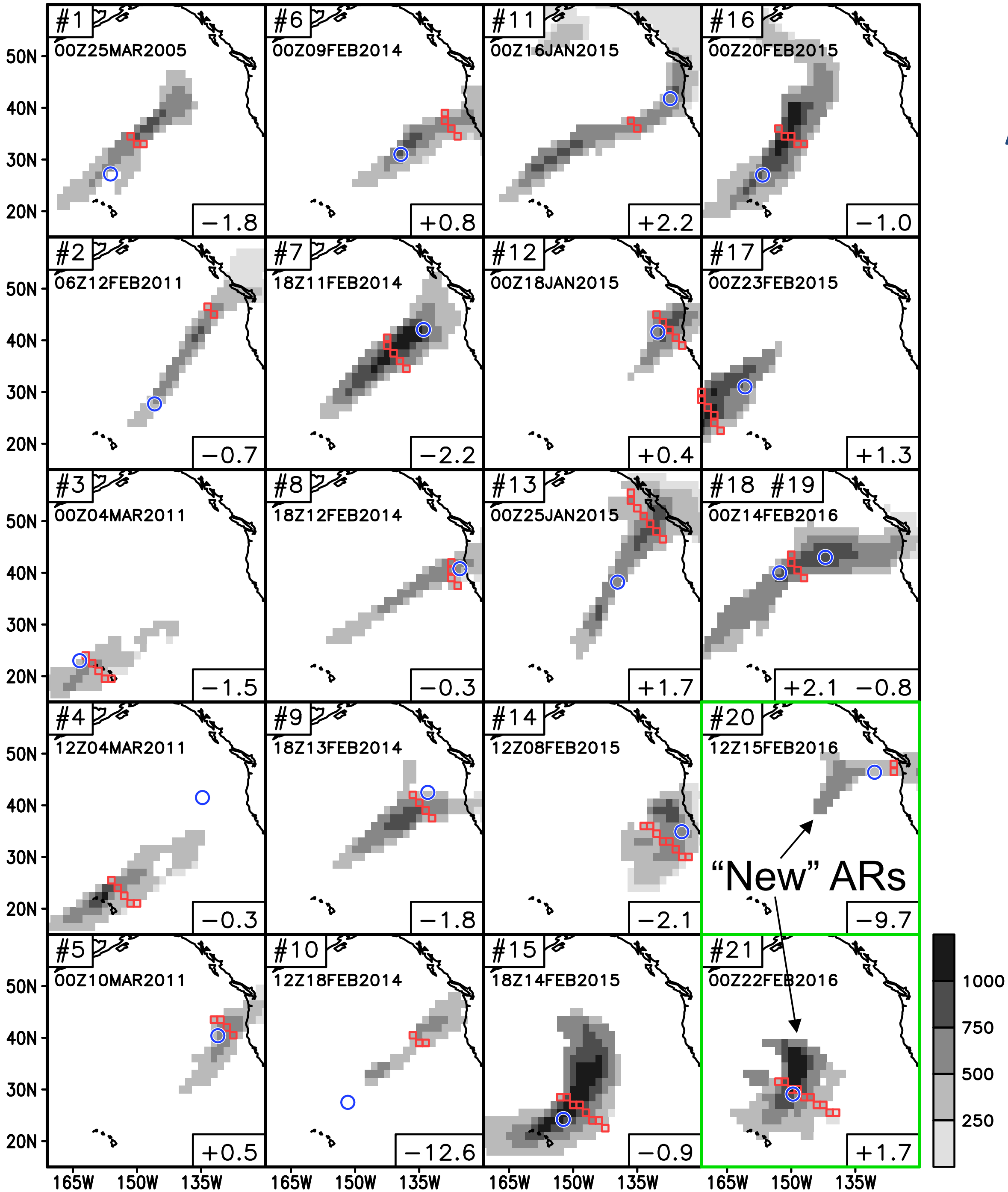

Algorithm captures 21 dropsonde-observed ARs

Algorithm + Reanalysis

- Shading: AR shapes.
- Red: transect going through AR centroid.

Dropsonde

Blue: midpoint of AR transect.

All 21 dropsonde ARs have a matching reanalysis AR; 19 of them matched within ±3 hours.

20-year Simulations from Global Weather/Climate Models

GASS-YoTC Multi-model Experiment

Model Name	Native Resolution (Lon × Lat, # of Vertical Levels)	Remark
BCC-AGCM2.1	T42 (2.8°), L26	
ISUGCM	T42 (2.8°), L18	
SPCAM3	T42 (2.8°), L30	Super-parameterized, Daily Archive
UCSD-CAM3	T42 (2.8°), L26	
GISS-E2	2.5° × 2.0°, L40	
TAMU-CAM4	2.5° × 1.9°, L26	
FGOALS-s2	R42 (2.8° × 1.6°), L26	
ACCESS1	1.875° × 1.25°, L85	
MetUM-GA3	1.875° × 1.25°, L85	
MIROC5	T85 (1.5°), L40	
CNRM-AM	T127 (1.4°), L31	
EC-GEM	1.4°, L64	
MRI-AGCM3	T159 (1.125°), L48	
CAM5	1.25° × 0.9°, L30	
CAM5-ZM	1.25° × 0.9°, L30	
CFS2	T126 (1°), L64	
CWB-GFS	T119 (1°), L40	
ECEarth3	T255 (0.7°), L91	
GEOS5	0.625° × 0.5°, L72	
NavGEM1	T359 (0.42°), L42	
CanCM4	2.8°, L35	Coupled
SPCCSM3	T42 (2.8°), L30	Coupled, Super-parameterized, Daily Archive
ECHAM5-SIT	T63 (2°), L31	Coupled
ECHAM6	T63 (2°), L47	Coupled

Grid cell size

Atmos.-only

Coupled

Weather/Climate Simulations of ARs

Process Level Considerations & Water Budget

$$\text{IWV Tendency} = \text{IVT Convergence} + \text{Evap} - \text{Precip}$$

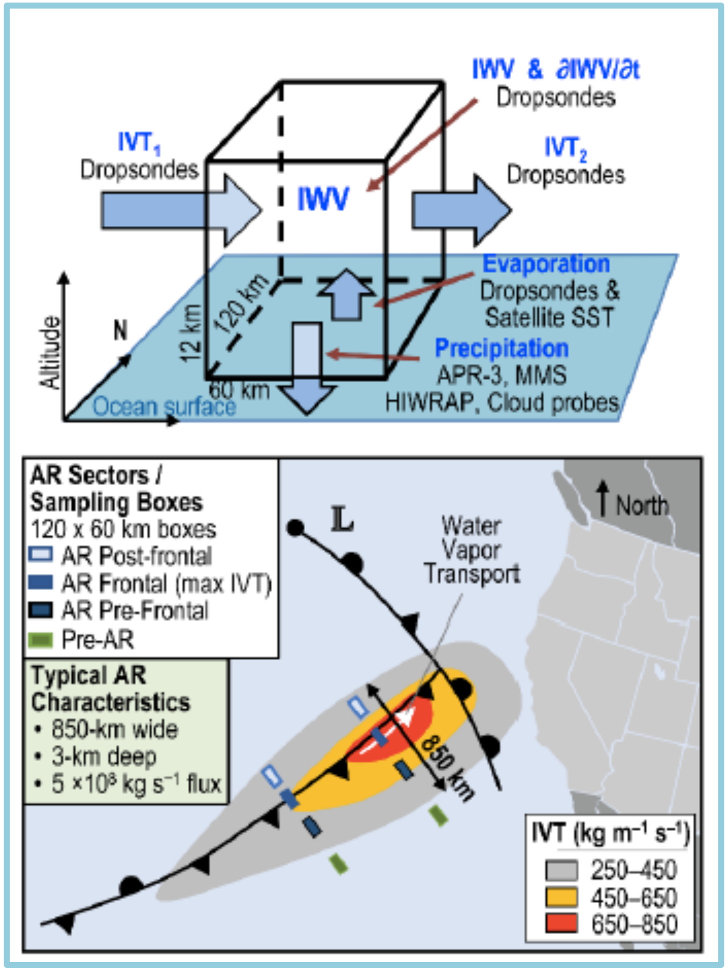

Figure Courtesy of CW3E/Ralph

Weather/Climate Simulations of ARs

Process Level Considerations & Water Budget

IWV Tendency = IVT Convergence + Evap − Precip

$$\frac{\partial}{\partial t}\int_0^{p_s} q\,dp = -\int_0^{p_s}(\underbrace{\mathbf{u}\cdot\nabla q}_{1} + \underbrace{q\nabla\cdot\mathbf{u}}_{2})\,dp - \underbrace{q_s\mathbf{u_s}\cdot\nabla p_s}_{3} + E - P$$

IVT Convergence due to

1. Moisture Advection
2. Mass Convergence
3. Surface process

Adapted from Eqn. 15 of Seager & Henderson (2013)

Reanalyses

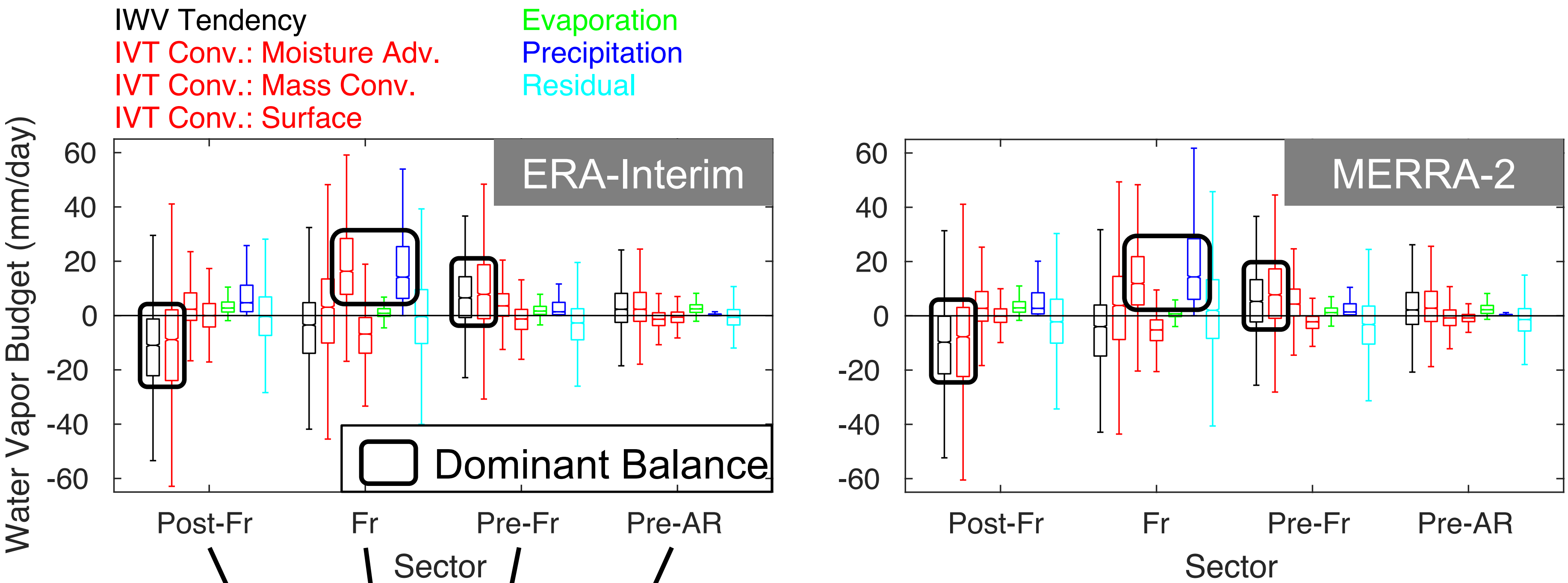

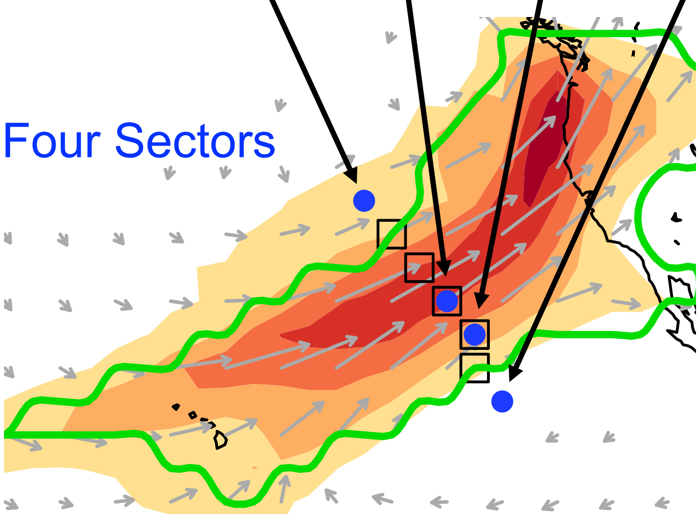

- Based on ~6000 ARs detected over northeastern Pacific during 1991-2010 NDJFM
- Overall, good agreement between ERA-Interim and MERRA-2
- Each sector of the four is unique relative to the others, with water budget dominated by different terms

Individual Models

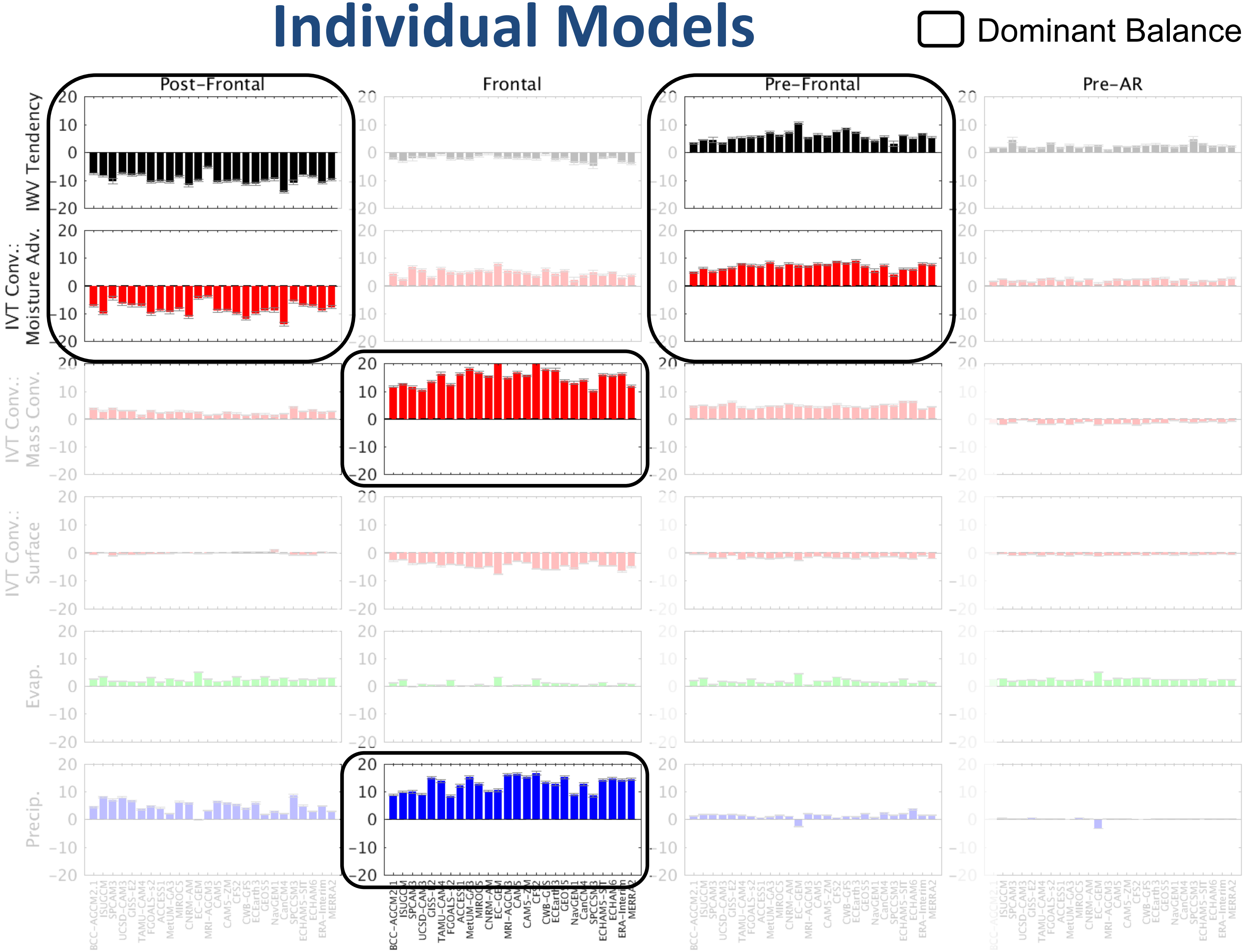

Model Spread

- Model spread (box-whiskers) is notable compared to observational uncertainty (diff. between two circles)
- Largest model spread occurs in post-frontal and frontal sectors in their respective dominant budget terms
- Largest observational uncertainty is associated with IVT convergence due to mass convergence in frontal sector

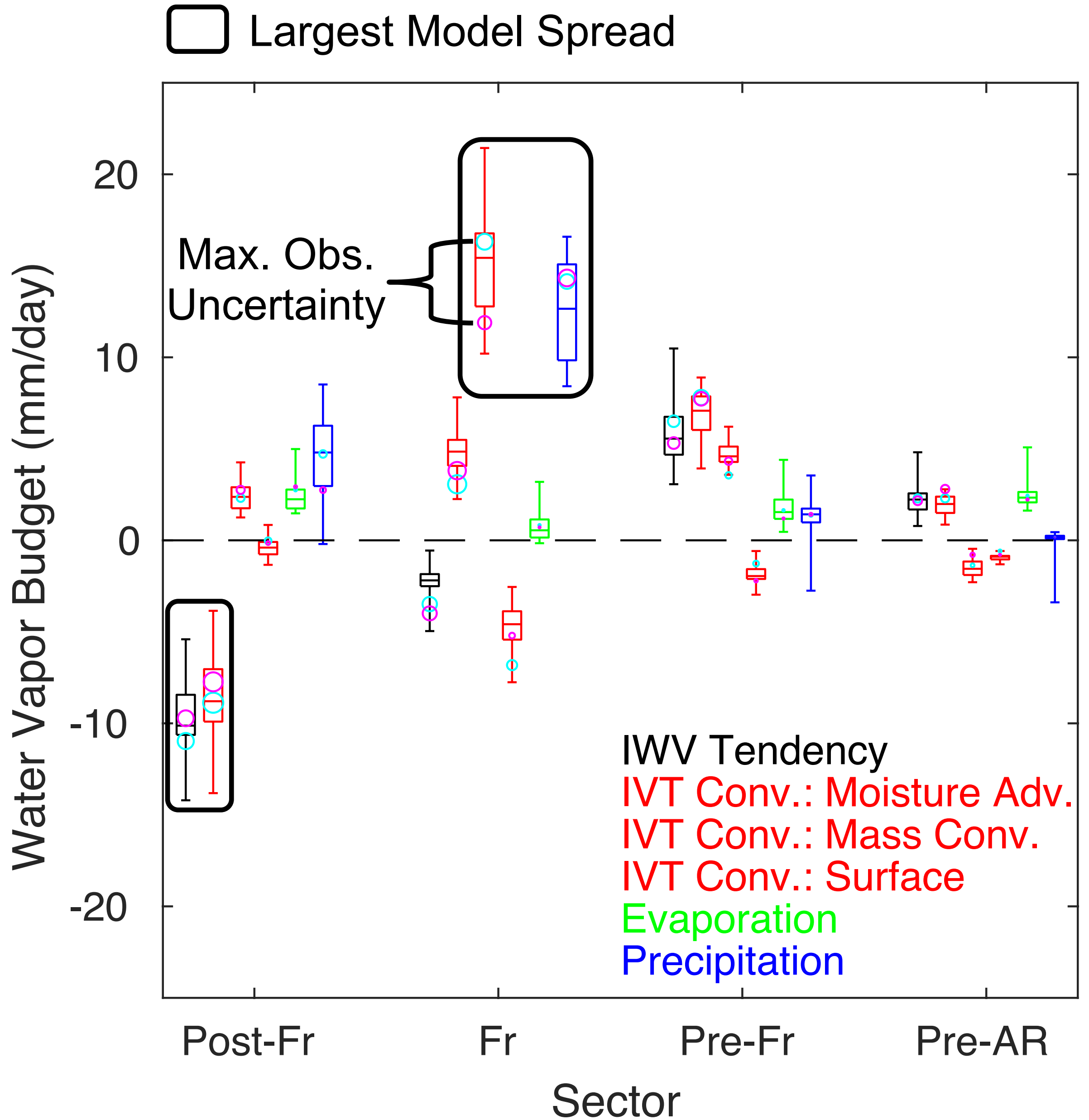

Relating water budget biases to model fidelity in bulk AR characteristics

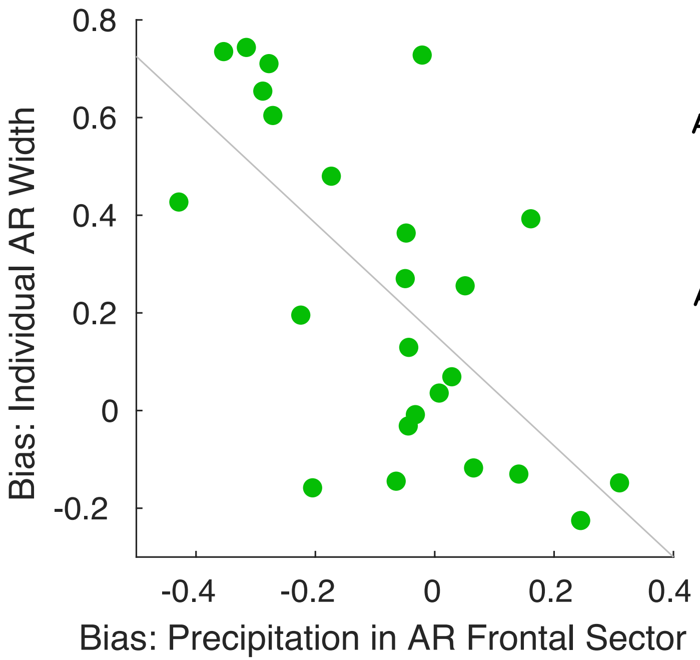

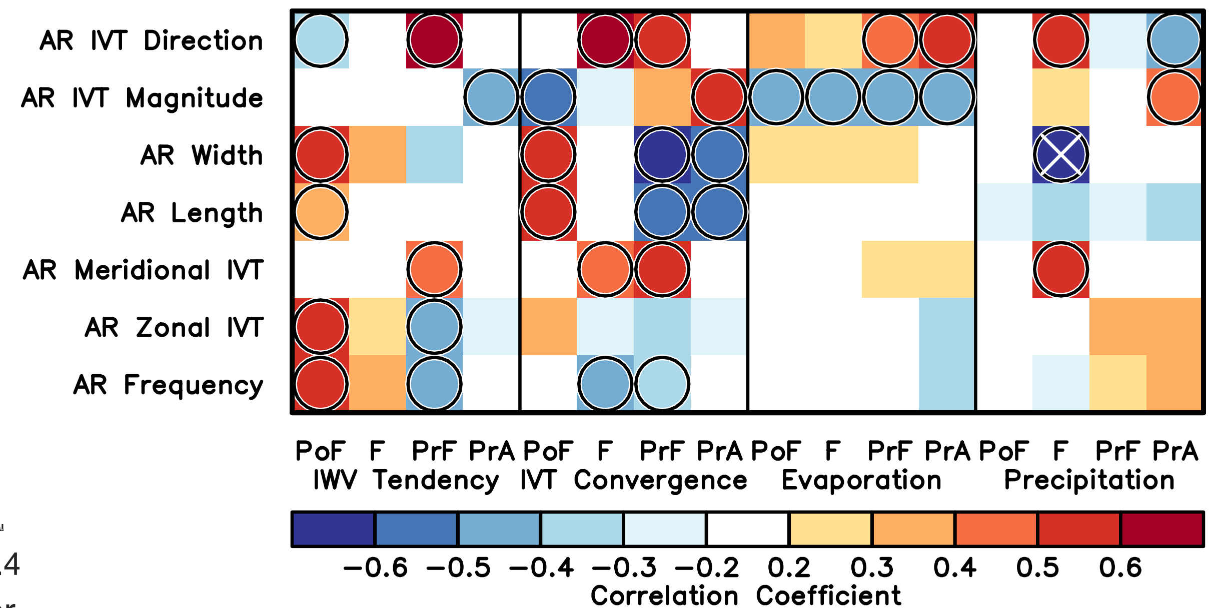

- Example (left): Too much precipitation in AR frontal sector (i.e., bias in water budget) is related to too narrow ARs (i.e., bias in bulk AR characteristics)
- Examination of 4 terms @ 4 sectors and 7 bulk AR characteristics (right) indicates simulated bulk AR characteristics overall have larger sensitivity to biases in IVT convergence and IWV tendency compared to E/P (counting # of circles, i.e., significant correlations)

Correlations Between Water Budget Terms: Reanalyses

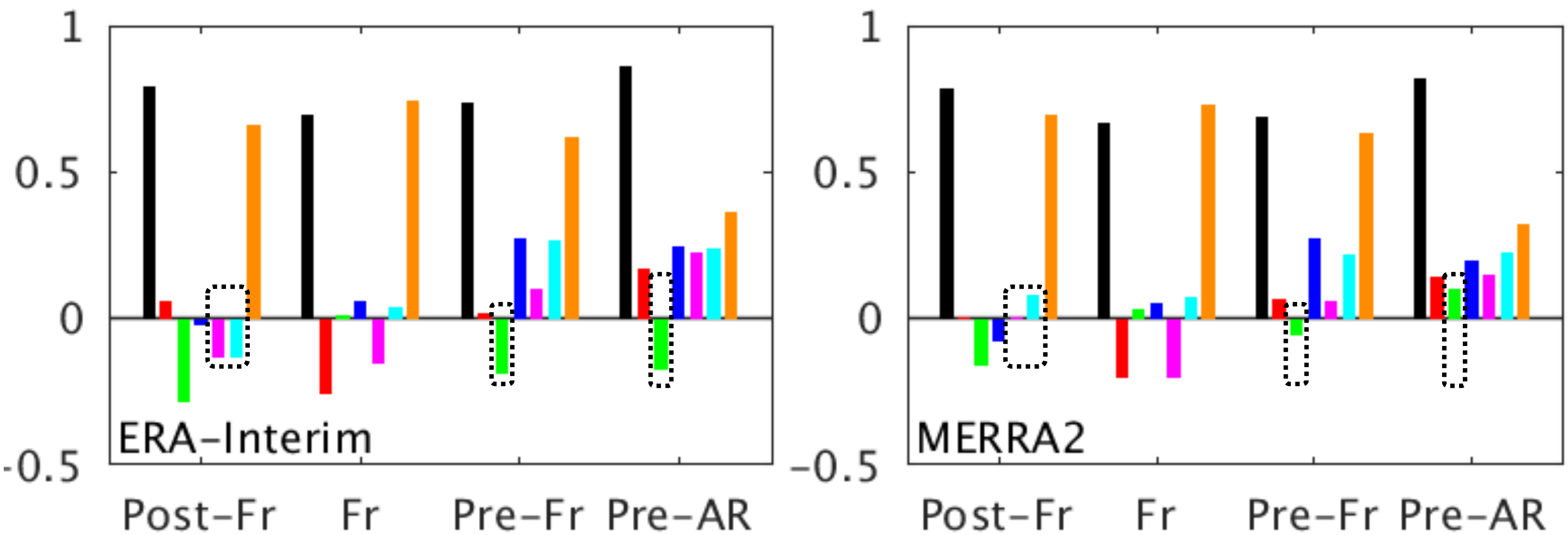

r(dIWV/dt, IVT Conv. due to Moisture Advection)
r(dIWV/dt, IVT Conv. due to Mass Convergence)
r(dIWV/dt, IVT Conv. due to Surface Process)
r(dIWV/dt, Evap.)
r(dIWV/dt, Precip.)

r(Precip., IVT Conv. due to Moisture Advection)
r(Precip., IVT Conv. due to Mass Convergence)

- Good agreement between ERA-Interim and MERRA-2 with a few exceptions (as marked)
- Each sector of the four is unique relative to the others, with correlation dominated by different terms

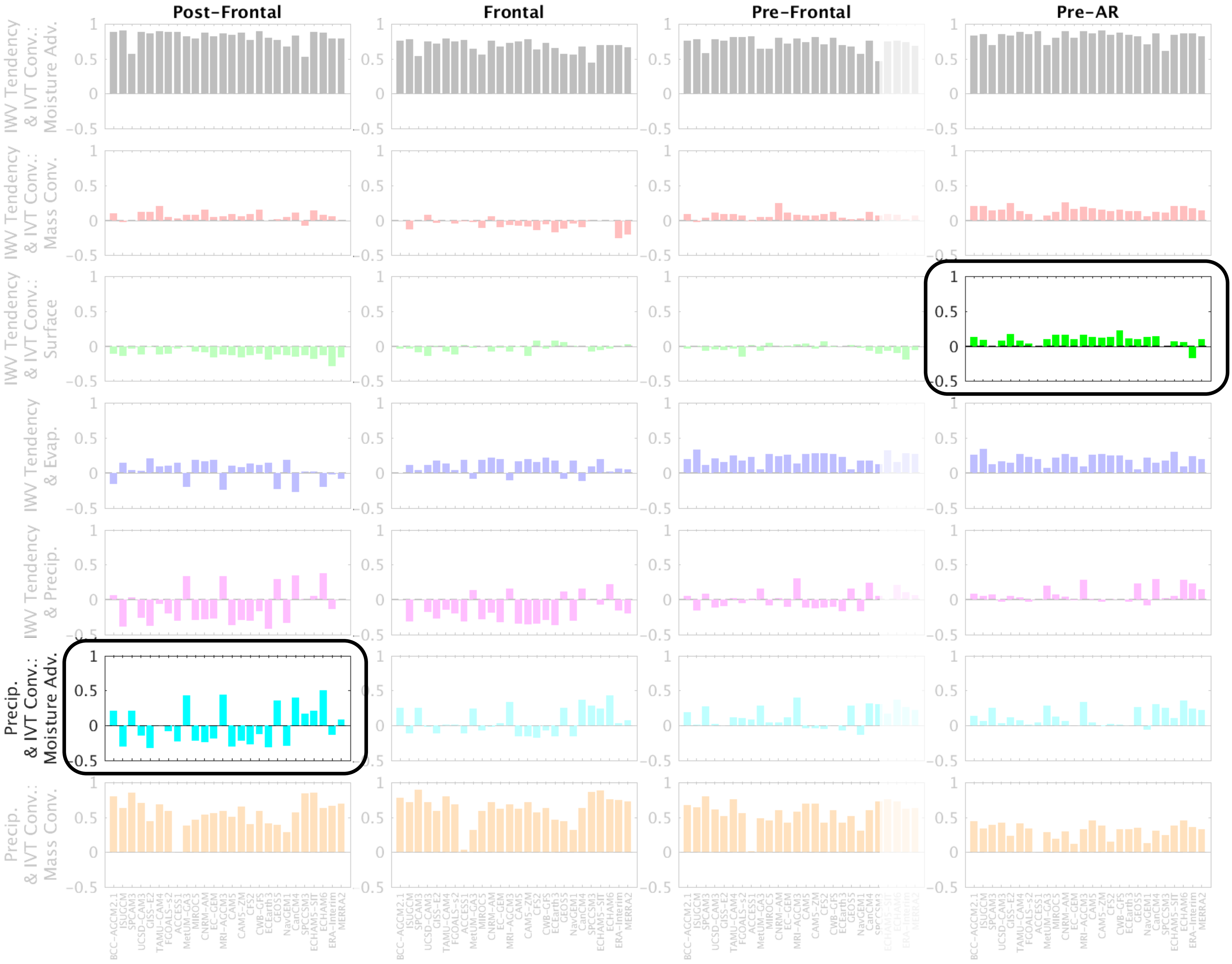

Post−Frontal
Frontal
Pre−Frontal
Pre−AR
IWV Tendency & IVT Conv.: Moisture Adv.
IWV Tendency & IVT Conv.: Mass Conv.
IWV Tendency & IVT Conv.: Surface
IWV Tendency & Evap.
IWV Tendency & Precip.
Precip. & IVT Conv.: Moisture Adv.
Precip. & IVT Conv.: Mass Conv.
1
0.5
0
−0.5
BCC-AGCM2.1
ISUGCM
SPCAM3
UCSD-CAM3
GISS-E2
TAMU-CAM4
FGOALS-s2
ACCESS1
MetUM-GA3
MIROC5
CNRM-AM
EC-GEM
MRI-AGCM3
CAM5
CAM5-ZM
CFS2
CWB-GFS
ECEarth3
GEOS5
NavGEM1
CanCM4
SPCCSM3
ECHAM5-SIT
ECHAM6
ERA-Interim
MERRA2

Summary

- The Guan and Waliser (2015) global AR detection algorithm is refined and applied to 20-year, 6-hourly simulations by 24 global weather/climate models;
- Water budget terms in four sectors of each AR were extracted from ~6000 wintertime ARs in the northeastern Pacific;
- **Model biases** in AR water budget are evaluated against two reanalysis products; the results reveal
  - **dominant water balance is different across the four AR sectors;**
  - **largest inter-model spread is associated with the dominant budget terms in the frontal and post-frontal sectors;**
- **Observational uncertainties** (i.e., reanalysis discrepancies) include
  - **IVT convergence due to mass convergence in frontal sector;**
  - **sign of correlation between precipitation and IVT convergence due to moisture advection in post-frontal sector;**
- Coordinated observational and modeling efforts are needed to better characterize and constraint AR water budget for better simulation/prediction of ARs.